Experimental Discovery of Double-Dirac Materials and its Physical Property Characterizations

Xin Zhang

2020 PARADIM REU Intern @ Johns Hopkins University

Intern Affiliation: Chemical and Biomolecular Engineering, Johns Hopkins University

Program: 2020 Platform for the Accelerated Realization, Analysis, and Discovery of Interface Materials Research Experience for Undergraduates Program at Johns Hopkins University

JHU REU Principal Investigator: Prof. Tyrel M. McQueen, Chemistry, Physics and Astronomy, and Materials Science and Engineering, Johns Hopkins University

JHU REU Mentor: Tanya Berry, Chemistry, Johns Hopkins University

Primary Source of JHU REU Funding: Support for PARADIM is provided under NSF Grant # DMR-1539918 as part of the Materials Innovation Platform Program

Contact: xzhan206@jhu.edu, paradim@jhu.edu

Website: https://www.paradim.org/reu/jhu

*Primary JHU PARADIM Tools Used: Origin La*b

Abstract:

Dirac materials are materials that have a linear band crossing in energy-momentum space, which forms a Dirac point with a 4-fold degeneracy. These types of materials are known to have high electron mobility, making it appealing for electronic applications. A big difference between Dirac and double-Dirac materials is that double-Dirac materials have an 8-fold degeneracy, rather than 4. The properties of double-Dirac materials were recently discovered in recent publications, although finding suitable candidates for double-Dirac materials is difficult, due to its specific symmetry constraints. However, $EuPd_3S_4$ and $LaPd_3S_4$ were discovered to be double-Dirac candidates. The focus of this project is to utilize heat capacity data to help realize its physical property characterizations, specifically heat capacity itself, entropy, and its critical exponents. The next step is to utilize neutron diffraction data for these materials for further insight into their realizations.

Summary of Research:

Background. Double-Dirac materials have specific symmetry constraints, which makes it difficult to find suitable candidates. Additionally, finding metallic double-Dirac candidates increases this difficulty, as there needs to be a small number of bands crossing at the Fermi energy. These materials need to have a non-symmorphic space group, which out of the 230 known space groups, 157 are non-symmorphic. However, out of those 157 space groups, only 7 of these space groups can allow a compound to be double-Dirac. $EuPd_3S_4$ and $LaPd_3S_4$ are double-Dirac materials with a cubic crystal structure and space group 223 Pm-3n. The difference between the two compounds is their magnetic properties. For $LaPd_3S_4$, La^{3+} makes the material non-magnetic. For EuPd3S4, there is a 50/50 split of Eu^{2+} and Eu^{3+}, making the material magnetic as noted by Mössbauer spectroscopy and Curie Weiss analysis. It is unknown if the magnetic structure of $EuPd_3S_4$ is the same as its crystal structure. Heat capacity data for both compounds are needed to understand this. The data was acquired through PPMS (Physical Properties Measurement System).

Heat Capacity. Heat Capacity data is useful in determining a material's magnetic properties, and it can be processed to determine its entropy and critical exponents. In Figure 1, a phase transition occurs at $\mu_o H$=0T to 2T, where $EuPd_3S_4$ transitions from a paramagnetic state to an antiferromagnetic state as temperature decreases. At 5 and 9 Tesla, there is no phase transition, where it matches similarly to the heat capacity data of $LaPd_3S_4$ (Figure 2), a non-magnetic material. There is a noticeable trend: with increasing field, the phase transition occurs at lower temperatures until 5 Tesla, where no phase transition occurs.

Entropy. Determining the spin-system of $EuPd_3S_4$ is done through processing heat capacity to be in units of entropy.

$$S = \int_{T_o}^{T} \frac{C_p}{T} dT \quad (1)$$

$$S = Rln(2(Spin) + 1) \quad (2)$$

Integrating a CpT^{-1}/T graph creates an Entropy vs Temperature graph, according to equation 1 [1]. Before integrating, the phonon contributions are subtracted from $EuPd_3S_4$ using the heat capacity data from $LaPd_3S_4$ (since $LaPd_3S_4$ is non-magnetic). For $EuPd_3S_4$, Eu^{2+} has a theoretical max of a spin 7/2 system. Though in Figure 3, it can be seen that the entropy values closely match a spin 1/2 system. There are a variety of reasons as to why this might be the case, although would require neutron diffraction data in order to exactly understand why.

Critical Exponent. Critical exponents are used to describe the behavior of physical quantities near continuous phase

transitions. For heat capacity, the critical exponent α is used.

$$\alpha = \lim_{\tau \to 0} \frac{log|f(\tau)|}{log|\tau|}, \; where \; \tau = \frac{T}{T_N} - 1 \; (3)$$

$$For \; \tau > 0: C \propto \tau^{-\alpha} \; (4)$$

$$For \; \tau < 0: C \propto \tau^{-\alpha'} \; (5)$$

For heat capacity, two α values were calculated (Equation 4,5 [2]) by first making a graph of heat capacity over $|\tau|$, where it is converted to a log scale. The α value is then calculated by taking the linear regression as close to the critical temperature as possible, where the selected range was approximately 5% from the selected critical temperatures for each field value. The α value is matched with another α value that best fits a particular universality class (Table 3), which determines the behavior of a material's magnetic structure as it approaches its critical temperature.

Future Work:

The next part of this project is to compare the data from heat capacity with neutron diffraction data specifically to compare critical exponent values (α for heat capacity, and β for intensity values from neutron diffraction). In addition, the neutron diffraction data will be used to determine the reason for the low spin system from the entropy data. Additionally, to have a higher confidence in the calculated α values from heat capacity, the $EuPd_3S_4$ sample will be analyzed again through PPMS, at a temperature range closer to its critical temperatures.

Acknowledgements:

Funding for this project is supported by the NSF (Platform for the Accelerated Realization, Analysis and Discovery of Interface Materials (PARADIM)) under Cooperative Agreement No. DMR-1539918 as part of the Materials Innovation Platform Program.

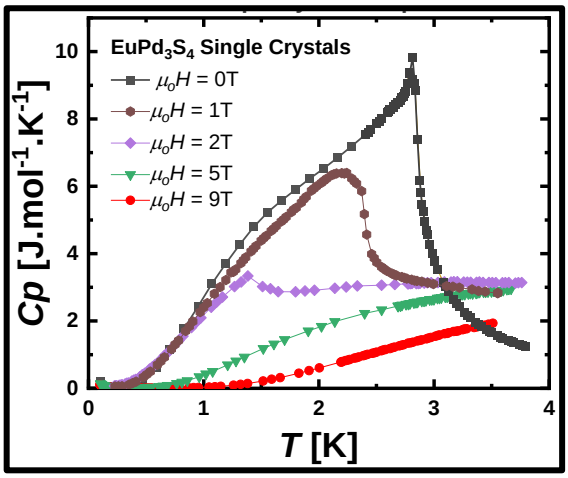

Figure 1: Heat Capacity vs. Temperature graph for $EuPd_3S_4$. Phase transitions occur at T≈2.8K for 0 T, T≈2.3K for 1 T, and T≈1.4K for 1 T. At 5 T and 9 T, the phase transition disappears.

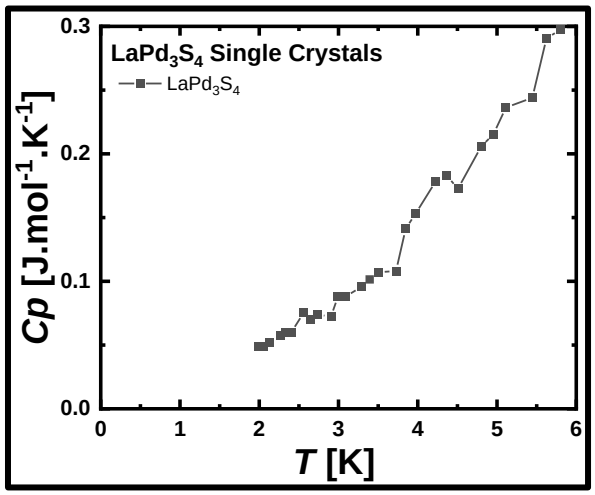

Figure 2: $LaPd_3S_4$ has a linear trend as temperature increases, as the material is nonmagnetic.

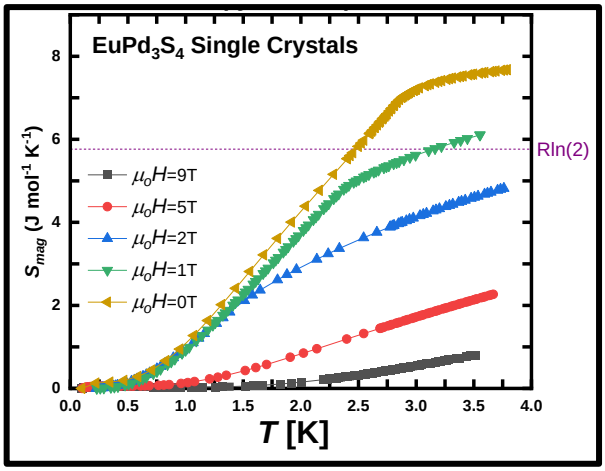

Figure 3: Entropy vs. Temperature graph for $EuPd_3S_4$. Entropy values match closest to a spin 1/2 system, far from the theoretical max of the 7/2 spin system, as predicted Eu^{2+}

$EuPd_3S_4$	Above T_N	Below T_N
0 Tesla	$\alpha \approx .45$ -2D Directed Percolation $-1 - Dih_4$	$\alpha \approx .07$ -3D Ising $-Sym_2, Oct$
1 Tesla	$\alpha \approx .1256$ -3D Ising $- Sym_2, Oct$	$\alpha \approx .1256$ -3D Heisenberg or 3D XY $- O(3)$ *or* $O(2), Oct$
2 Tesla	$\alpha \approx .102$ -3D Ising $-Sym_2, Oct$	$\alpha \approx .32$ -2D 3-State Potts $-Sym_3, Dih_4$

Table 1: A table of calculated α critical exponents under varying fields, and their corresponding universality classes [2].

References:

[1] Tari, A. (2003). The Specific Heat of Matter at Low Temperatures. In *The Specific Heat of Matter at Low Temperatures* (1st ed., pp. 2-9) Imperial College Press.

[2] Ma, S. (2000). *Modern Theory of Critical Phenomena* (1st ed.). Routledge.

[3] Bradlyn, B., J. Cano, Z. Wang, M. Vergniory, C. Felser,R. Cava, and B. A. Bernevig, 2016, Science353(6299),aaf503.